

Hetero-Motif Molecular Junction Photocatalysts: A New Frontier in Artificial Photosynthesis

Lei Zhang, Jiang Liu, and Ya-Qian Lan*



Cite This: <https://doi.org/10.1021/acs.accounts.3c00751>



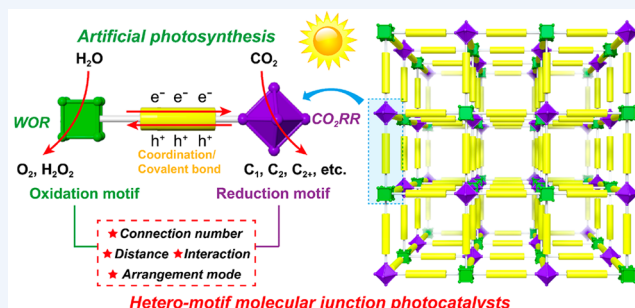
Read Online

ACCESS |

Metrics & More

Article Recommendations

CONSPECTUS: To cope with the increasingly global greenhouse effect and energy shortage, it is urgent to develop a feasible means to convert anthropogenic excess carbon dioxide (CO_2) into energy resources. The photocatalytic CO_2 reduction reaction (CO_2RR) coupled with the water oxidation reaction (WOR), known as artificial photosynthesis, is a green, clean, and promoting strategy to deal with the above issues. Among the reported photocatalytic systems for CO_2 reduction, the main challenge is to achieve WOR simultaneously due to the limited charge separation efficiency and complicated dynamic process. To address the problem, scientists have assembled two nanosemiconductor motifs for CO_2RR and WOR into a heterojunction photocatalyst to realize artificial photosynthesis. However, it is difficult to clearly explore the corresponding catalytic mechanism and establish an accurate structure–activity relationship at the molecular level for their aperiodic distribution and complicated structural information. Standing on the shoulders of the heterojunction photocatalysts, a new-generation material, hetero-motif molecular junction (HMMJ) photocatalysts, has been developed and studied by our laboratory. A hetero-motif molecular junction is a class of crystalline materials with a well-defined and periodic structure, adjustable assembly mode, and semiconductor-like properties, which is composed of two predesigned motifs with oxidation and reduction, respectively, by coordination or covalent bonds. The intrinsic properties make these catalysts susceptible to functional modifications to improve light absorption and electrical conductivity. The small size and short distance of the motifs can greatly promote the efficiency of photogenerated electron–hole separation and migration. Based on these advantages, they can be used as potential excellent photocatalysts for artificial photosynthesis. Notably, the explicit structural information determined by single-crystal or powder X-ray diffraction can provide a visual platform to explore the reaction mechanism. More importantly, the connection number, spatial distance, interaction, and arrangement mode of the structural motifs can be well-designed to explore the detailed structure–activity relationship that can be hardly studied in nanoheterojunction photocatalyst systems. In this regard, HMMJ photocatalysts can be a new frontier in artificial photosynthesis and serve as an important bridge between molecular photocatalysts and solid photocatalysts. Thus, it is very important to summarize the state-of-the-art of the HMMJ photocatalysts used for artificial photosynthesis and to give in-depth insight to promote future development.



In this Account, we have summarized the recent advances in artificial photosynthesis using HMMJ photocatalysts, mainly focusing on the results in our lab. We present an overview of current knowledge about developed photocatalytic systems for artificial photosynthesis, introduce the design schemes of the HMMJ photocatalysts and their unique advantages as compared to other photocatalysts, summarize the construction strategies of HMMJ photocatalysts and their application in artificial photosynthesis, and explain why hetero-motif molecular junctions can be promising photocatalysts and show that they provide a powerful platform for studying photocatalysis. The structure–activity relationship and charge separation dynamics are illustrated. Finally, we bring our outlook on present challenges and future development of HMMJ photocatalysts and their potential application prospects on other photocatalytic reaction systems. We believe that this Account will afford important insights for the construction of high-efficiency photocatalysts and guidance for the development of more photocatalytic systems in an atom-economic, environmentally friendly, and sustainable way.

KEY REFERENCES

- Zhang, L.; Li, R.-H.; Li, X.-X.; Liu, J.; Guan, W.; Dong, L.-Z.; Li, S.-L.; Lan, Y.-Q. Molecular oxidation–reduction junctions for artificial photosynthetic overall reaction. *Proc. Natl. Acad. Sci. U.S.A.* **2022**, *119*, e2210550119.¹

Received: November 28, 2023

Revised: February 9, 2024

Accepted: February 12, 2024



ACS Publications

© XXXX American Chemical Society

A

<https://doi.org/10.1021/acs.accounts.3c00751>
Acc. Chem. Res. XXXX, XXX, XXX–XXX

This key reference presents the concept of hetero-motif molecular junction photocatalysts and revealed that the arrangement between oxidation and reduction motifs can affect the orbital distribution and energy level of the catalysts, and then make an impact on the photocatalytic performance.

- Zhou, J.; Li, J.; Kan, L.; Zhang, L.; Huang, Q.; Yan, Y.; Chen, Y.; Liu, J.; Li, S.-L.; Lan, Y.-Q. Linking oxidative and reductive clusters to prepare crystalline porous catalysts for photocatalytic CO₂ reduction with H₂O. *Nat. Commun.* **2022**, *13*, 4681.² This key reference reports the preparation of hetero-motif molecular junction photocatalysts by covalently linking oxidative and reductive clusters. The constructed MCOF-Ti₆Cu₃ photocatalyst exhibits fine activity in the conversion of CO₂ with water into HCOOH.
- Lu, M.; Zhang, M.; Liu, J.; Yu, T.-Y.; Chang, J.-N.; Shang, L.-J.; Li, S.-L.; Lan, Y.-Q. Confining and Highly Dispersing Single Polyoxometalate Clusters in Covalent Organic Frameworks by Covalent Linkages for CO₂ Photoreduction. *J. Am. Chem. Soc.* **2022**, *144*, 1861–1871.³ This key reference reports a strategy for uniformly dispersed reductive polyoxometalates in oxidative covalent-organic frameworks. The constructed TCOF-MnMo₆ photocatalyst exhibits outstanding catalytic activity in artificial photosynthesis in a gas–solid reaction system.
- Dong, L.-Z.; Zhang, L.; Liu, J.; Huang, Q.; Lu, M.; Ji, W.-X.; Lan, Y.-Q. Stable Heterometallic Cluster-Based Organic Framework Catalysts for Artificial Photosynthesis. *Angew. Chem., Int. Ed.* **2020**, *59*, 2659–2663.⁴ This key reference reports a series of stable heterometallic Fe₂M cluster-based metal–organic frameworks (MOFs) to achieve the overall conversion of CO₂ and H₂O into HCOOH (selectivity of ca. 100%) and O₂.

1. INTRODUCTION

Due to severe environmental and energy issues, carbon neutrality has become a hot topic around the world.^{5–11} By simulating the natural photosynthesis of green plants, artificial photosynthesis, coupled with the carbon dioxide reduction reaction (CO₂RR) and the water oxidation reaction (WOR), has become one of the most important and sustainable means to achieve this goal.^{12–15} It not only achieves a green conversion of CO₂ and water to fossil fuels, but also avoids some of the drawbacks of the individual CO₂RR and WOR half-reaction systems, such as high cost, low atom economy, and potential environmental problems for additional photosensitizers and sacrificial agents. The most optimal system of artificial photosynthesis only consists of light, water, CO₂, and photocatalyst, in which the efficient and stable photocatalyst is the core of the system. The whole catalytic process can be simplified as follows. First, the photocatalyst is excited and produces photogenerated electrons and holes under light irradiation. Subsequently, electrons and holes separate and migrate to the reduction and oxidation sites, respectively, and react with adsorbed CO₂ and water molecules. Water molecules then are oxidized to O₂ or hydrogen peroxide (H₂O₂) and provide protons and electrons for reducing CO₂ to CO or hydrocarbons (HCOOH, CH₄, C₂H₄, etc.). Since the simultaneous progress of the two half-reactions requires both photogenerated electrons and holes to have strong energy, wide-bandgap semiconductor

photocatalysts are required to ensure a large energy difference between electrons and holes and match the potentials of CO₂RR and WOR simultaneously. However, such photocatalysts usually need high-energy blue-violet or even ultraviolet light to achieve the excitation and separation of electron–hole pairs and suffer from the subsequently rapid electron–hole recombination.¹⁶ How to improve the separation of photogenerated electrons and holes to suppress recombination is one of the key factors.^{17,18} However, there is a lack of well-defined molecular models to explore the precise structure–activity relationship, especially involving the molecular-level regulation of active motifs for CO₂RR and WOR.

For the first question, the researchers proposed to combine two kinds of semiconductors to construct heterojunction photocatalysts.^{19,20} Because of the matching band structures, the photogenerated electrons and holes can migrate to two semiconductors, respectively, thus inhibiting the electron–hole recombination. Due to the improved separation efficiency of the photogenerated charges and separated catalytic sites for CO₂RR and WOR, respectively, heterojunction photocatalysts were used to accomplish artificial photosynthesis.^{21–23} However, the large size of the nanosemiconductors and the limited total contact area could hinder the further improvement of photocatalytic reactivity.²⁴ In addition, such multiphase heterojunction materials make it difficult to achieve a precisely structural adjustment of period distribution, ratio, distance, interaction, and arrangement mode on the oxidative and reductive motifs. Inspired by the design concept of heterojunctions, recently, hetero-motif molecular junction (HMMJ) photocatalysts have been proposed and developed by our lab to realize artificial photosynthesis. HMMJ photocatalysts are a novel kind of crystalline materials constructed by connecting predesigned oxidative and reductive structural motifs with well-matched energy level structures through coordination bonds or covalent bonds (Figure 1). This new frontier of molecular-level photocatalyst can theoretically achieve precise assembly of a variety of structural motifs (photosensitive, oxidative, reductive motifs, etc.) in one long-ordered structure, as well as the precise control of the parameters such as the types, numbers, connection modes, connection numbers, and interactions of structural motifs. HMMJ photocatalysts not only have the advantages of heterojunction photocatalysts, but also have well-defined crystal structures to facilitate the construction of clear structure–performance relationships and provide theoretical guidance for guiding the synthesis of more artificial photosynthesis catalysts.

Toward the future development of HMMJ photocatalysts for artificial photosynthesis and more potential applications, this Accounts first presents the association and differences between HMMJ and semiconductor heterojunction photocatalysts. Next, two kinds of universal strategies to construct HMMJ photocatalysts and their respective advantages are introduced. Further, we place emphasis on the application of molecular junction photocatalysts in artificial photosynthesis, where the structure modification, activity adjustment, catalytic mechanism, and structure–activity relationship are included. In particular, the influence of the selection, connection mode, and spatial arrangement of the structure motifs on the separation and migration of photogenerated charges as well as the catalytic activity and stability of constructed photocatalysts are emphasized. Finally, we propose our perspectives on the challenges of HMMJ photocatalysts at the present stage and their broader application prospects in the future.

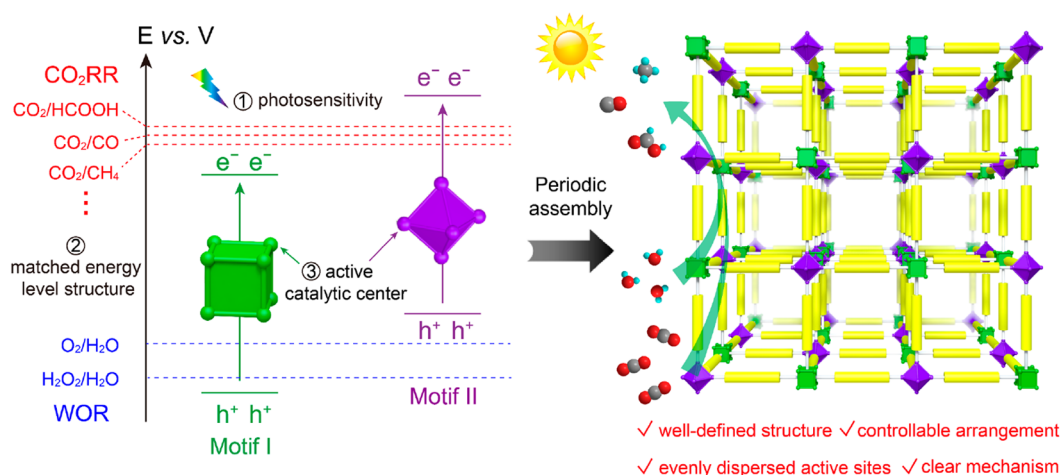


Figure 1. Design ideas for screening the appropriate structural motifs to construct hetero-motif molecular junction photocatalysts as well as the schematic representation for artificial photosynthesis.

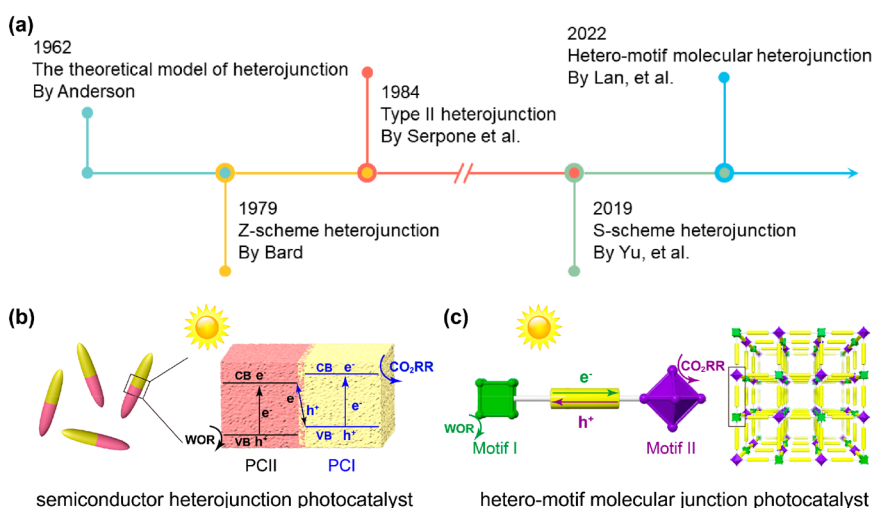


Figure 2. (a) Evolution timeline of the concepts for heterojunction and molecular junction photocatalysts. Operational mechanisms of artificial photosynthesis in (b) heterojunction catalysts and (c) HMMJ photocatalysts.

2. FROM SEMICONDUCTOR HETEROJUNCTION PHOTOCATALYSTS TO HETERO-MOTIF MOLECULAR JUNCTION PHOTOCATALYSTS

Heterojunction photocatalysts have been developed for more than half a century. Generally, a heterojunction is defined as the interface between two semiconductors with different energy band structures. According to the energy band structure and photogenerated charge transfer mode of the semiconductor motifs, there are several types of heterojunction photocatalysts, mainly including type II,^{25,26} Z-scheme,^{27,28} and S-scheme^{29,30} heterojunctions (Figure 2). Theoretically, the basic requirement for constructing an ideal heterojunction is to have matched lattice constants between structural motifs to reduce the interface defects and the recombination rate of photogenerated carriers. However, this makes certain limitations on the choice of semiconductors to construct heterojunctions. In contrast, hetero-motif molecular junction photocatalysts would be assembled with higher arbitrariness. Furthermore, HMMJ photocatalysts are crystalline materials with long-range ordering and well-defined structures from the assembly of molecular precursors (organics containing active centers, metal–oxo clusters, or metal–organic clusters) through coordination/

covalent linkage. The synthesized HMMJ photocatalysts can be characterized to obtain accurate crystal structures by single crystal X-ray diffraction (SCXRD) or powder X-ray diffraction (PXRD), which is conducive to probing the structure–property relationships at the molecular level. In addition, through different strategies such as direct bonding, grafted bonding, and postmodification, two or even more functionalized molecular motifs can be periodically arranged to achieve uniform dispersion of active sites. Such uniformly dispersed oxidation–reduction components in space can greatly improve the utilization of active sites. More importantly, the arrangement of molecular motifs is highly adjustable, enabling regulation of the energy level structures and internal photogenerated charge transfer of the photocatalyst. In this way, it becomes feasible to achieve discrepant photogenerated charge transfer modes in different HMMJ photocatalysts that are composed of the same motifs, which is difficult to be realized in semiconductor heterojunction photocatalysts and other composite materials. Therefore, the development of HMMJ photocatalysts can explore more structure–performance relationships that have been previously overlooked or not unearthed due to a lack of suitable molecular models.

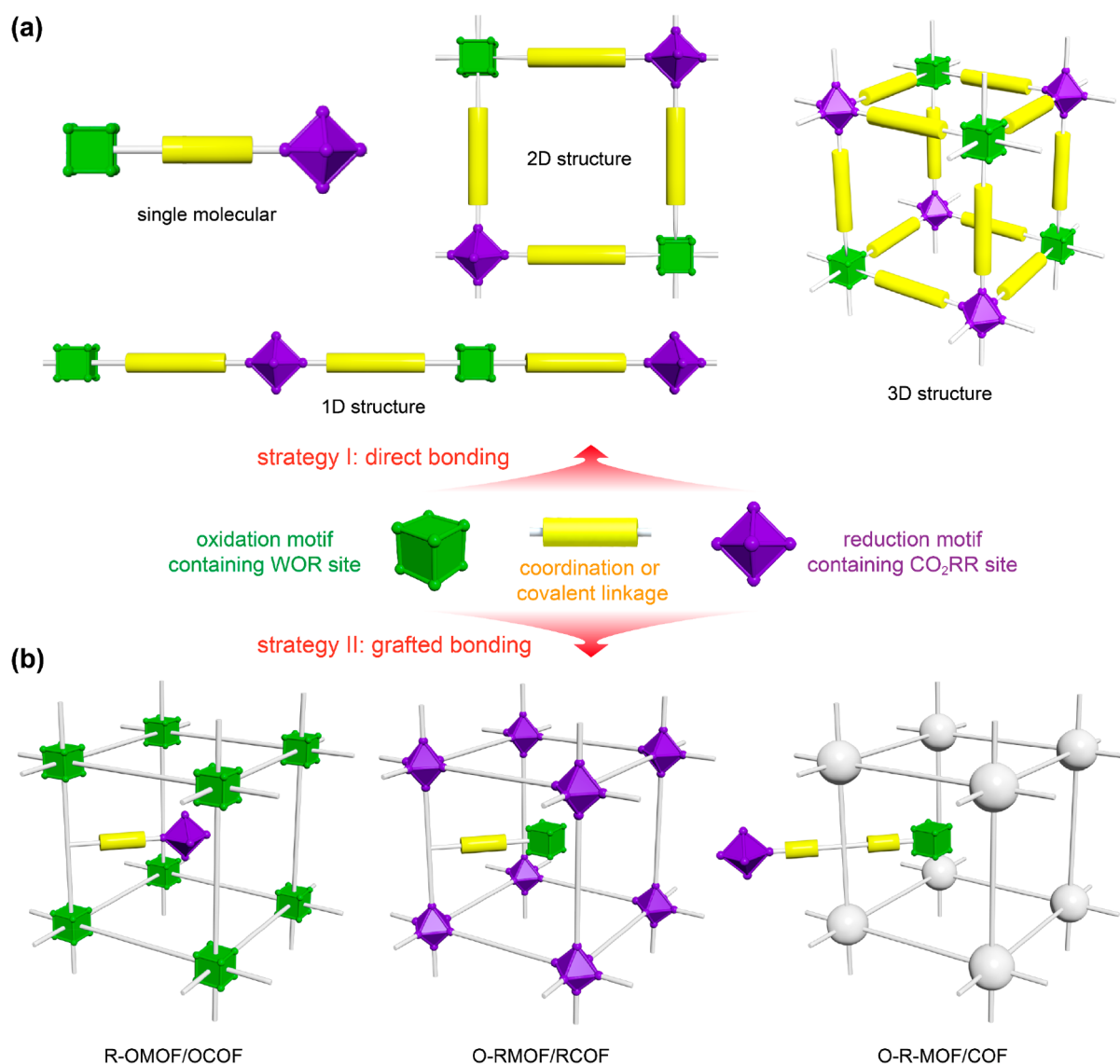


Figure 3. Two strategies for constructing HMMJ photocatalysts: (a) the direct bonding strategy and (b) the grafted bonding strategy.

In a molecular junction photocatalyst, the manner in which photogenerated charges separate and migrate between structural motifs is similar to that in semiconductor heterojunctions. Under illumination, two structural motifs are both excited and generate electron–hole pairs. Subsequently, due to the different electronic gain and loss capabilities of the two motifs, the photogenerated electrons on motif I can migrate and recombine with the holes of motif II. It allows the photogenerated electrons and holes to be located in different structural motifs, thus inhibiting the charge recombination. Next, reduction and oxidation sites with excited photogenerated electrons and holes achieve CO₂RR and WOR, respectively. There would be more charge migration modes in complicated molecular junction photocatalysts, which require specific analysis of different molecular models.

2.1. Design Schemes of the Hetero-Motif Molecular Junction Photocatalysts

In principle, to realize the above-mentioned process of artificial photosynthesis, construction of HMMJ photocatalysts needs to meet the following five requirements: (1) excellent light

absorption capacity, where the catalysts can be excited by light (preferably visible light or even near-infrared light) and generate electron–hole pairs; (2) at least two kinds of structural motifs to undertake CO₂RR and WOR, respectively; (3) the structural motifs can be assembled through chemical bonds; (4) a suitable energy level structure, highly active catalytic sites, and matching the reaction potential of CO₂RR and WOR; and (5) efficient separation and migration of photogenerated charges between CO₂RR and WOR motifs.

Fundamentally, selecting suitable reduction and oxidation motifs is the core of constructing molecular junction photocatalysts. Ideally, reduction and oxidation motifs could be prepared in advance. The advantage is that their energy level structures, including the lowest unoccupied molecular orbital (LUMO), the highest occupied molecular orbital (HOMO) positions, and the work function values, can be clearly evaluated by ultraviolet–visible–near-infrared (UV–vis–NIR) absorption spectroscopy, ultraviolet photoelectron spectroscopy (UPS), and Mott–Schottky plot characterizations.^{31,32} The values of the LUMO and HOMO positions can be also

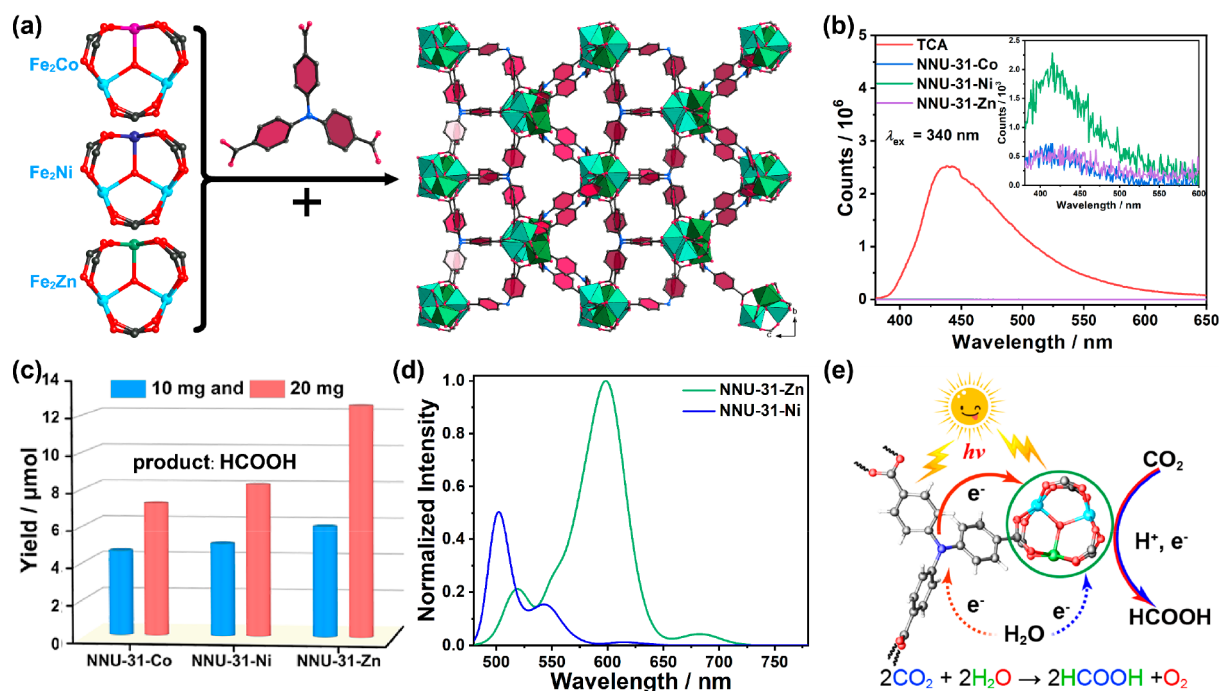


Figure 4. (a) The structure of NNU-31-M assembled from Fe_2M clusters and TCA ligands. (b) PL spectra of TCA ligand and NNU-31-M MOFs. (c) Photocatalytic performance of NNU-31-M for artificial photosynthesis. (d) Theoretical simulation light absorption of NNU-31-Zn and NNU-31-Ni. (e) Photocatalytic mechanism of artificial photosynthesis along with NNU-31-M MOFs as catalysts. Adapted with permission from ref 4. Copyright 2020 Wiley-VCH.

determined by cyclic voltammetry (CV) measurements.³³ The results of these characterizations also allow for the determination of the redox and electron-gaining/losing capacities of the reduction and oxidation motifs. A preliminary judgment then can be made as to whether effective charge transfer can occur between the reduction and oxidation motifs, and whether CO_2RR and WOR can be completed thermodynamically.

After selecting the appropriate motifs that have matched energy level structures, redox capacity, and active centers (for CO_2RR and WOR), the expected molecular junction photocatalyst can be constructed in the following two universal strategies. The first strategy is to connect the two motifs by coordination bonds or covalent bonds. The connection site can be a bridging atom/ligand or a new covalent bond formed by a chemical reaction (such as the Schiff base condensation reaction, Knoevenagel reaction, and Kröhnke oxidation reaction, etc.). Among them, it is easier to obtain products with a good crystalline state with the Schiff base condensation reaction. The $\text{sp}^2\text{C}=\text{C}$ bonds generated from the Knoevenagel reaction are more favorable for transferring photogenerated charges. According to the connection number of motifs, different types of molecular junction compounds can be obtained, such as single molecules, one or two-dimensional supramolecular structures, or three-dimensional frameworks (O-R-MOF or O-R-COF, Figure 3a). The adjustment of distance, proportion, and interaction between the reduction and oxidation motifs in the obtained molecular junction photocatalyst can be realized by customizing the geometry of the motifs and synthesis conditions. The second strategy is to beforehand construct a porous framework and then graft another kind of motif into the main structure through covalent or coordination bonds (O-RMOF/RCOF, R-OMOF/OCOF, or O-R-MOF/COF). This type of molecular junction photo-

catalysts has better structural predictability and can retain the original porosity of their host structures (Figure 3b).

3. HETERO-MOTIF MOLECULAR JUNCTION PHOTOCATALYSTS FOR ARTIFICIAL PHOTOSYNTHESIS

To understand the relationship between the structural tailorability of HMMJ photocatalysts and their photocatalytic performance, a series of HMMJ photocatalysts with different kinds of motifs and connection modes have been rationally constructed. Particularly, focusing on adjusting the active center species, the connection ratio and arrangement patterns between oxidation and reduction motifs, the separation and migration efficiency of photogenerated charges, and the impact on photocatalytic performance are carefully studied, which help to develop clear structure–performance relationships.

3.1. Coordination Assembly of Hetero-Motif Molecular Junction Photocatalysts

The heterometallic clusters containing both low- and high-valent metal ions have the active sites for both CO_2RR and WOR. Therefore, such heterometallic clusters can serve as the structural motifs to construct catalysts for artificial photosynthesis. However, isolated heterometallic clusters would face the problems such as poor light absorption, low water stability, and low porosity when used as photocatalysts. In this regard, connecting heterometallic clusters with photosensitive ligands to construct MOF can solve the above problems. Based on this idea, we assembled a series of stable heterometallic cluster-based MOFs (NNU-31-Zn/Co/Ni) from stable $\text{Fe}^{\text{III}}_2\text{M}^{\text{II}}$ ($\text{M} = \text{Ni}, \text{Co}, \text{or Zn}$) cluster precursors and photosensitive ligand 4,4',4''-tricarboxytriphenylamine (TCA), as shown in Figure 4a.⁴ Powder X-ray diffraction (PXRD) proves that the cluster-

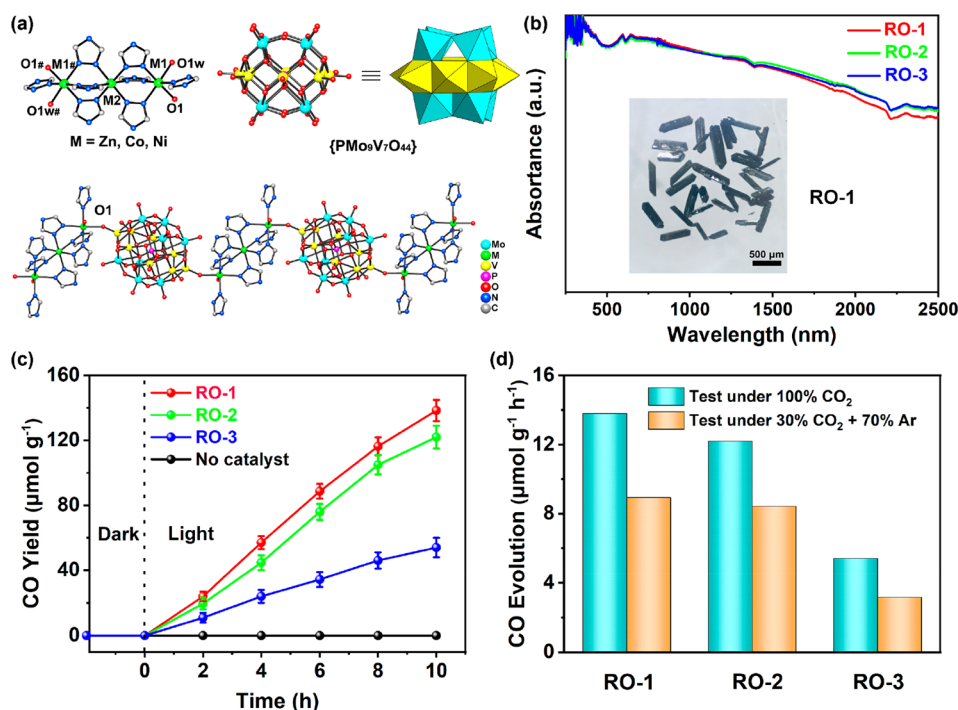


Figure 5. (a) Crystal structures and (b) UV–vis–NIR absorption spectra of **RO-1**, **-2**, and **-3**. (c) Photocatalytic performance of CO_2RR . (d) The comparison of the amount of produced CO along with **RO-1** as the photocatalyst. Adapted with permission from ref 37. Copyright 2021 American Chemical Society.

based MOFs have excellent water stability. Steady-state fluorescence spectroscopy (PL) results demonstrate that the connection between $\text{Fe}^{\text{III}}\text{M}^{\text{II}}$ cluster precursors and photosensitive TCA ligands can greatly promote the separation of photogenerated charges (Figure 4b). Thanks to the photosensitizer, and the reduction site and oxidation site that coexisted in the structure, this series of MOF catalysts realized the overall reaction process of photocatalytic CO_2 -to- HCOOH reduction coupling with H_2O -to- O_2 oxidation in water (Figure 4c). Among them, **NNU-31-Zn** exhibits the highest catalytic performance ($26.3 \mu\text{mol g}^{-1} \text{h}^{-1}$) and selectivity (ca. 100%). Density functional theory (DFT) calculations proved that the high-valence Fe^{III} ion is the active center for WOR, and the low-valence Zn^{II} site is responsible for CO_2RR (Figure 4d and e).

Placing the oxidation and reduction sites on different structural motifs can help to inhibit the recombination of photogenerated charges. It can be achieved by connecting two metal-based clusters to construct a heterocluster molecular-junction photocatalyst. Polyoxometalates (POMs) are a class of anionic metal-oxo clusters of early transition metal elements (Mo, W, V, Nb, and Ta). Multiple metal ions in POMs can bear multiple electron transfers for catalytic reactions. In addition, thanks to the strong redox ability and semiconductor-like properties of POMs, they have been widely used as photocatalytic CO_2RR and WOR catalysts.^{34–36} Furthermore, the surfaces of POMs are rich in terminal oxygen atoms and can introduce transition metal ions or organic ligands, which can make POMs be bonded with other types of metal-based clusters or grafted on a porous support to build HMMJ photocatalysts.

Phosphovanadomolybdates are a class of POMs with strong oxidizing properties, which is a strong candidate as an oxidation motif for building molecular junction photocatalysts. In this case, it is required that the reduction motifs need to remain open active sites for CO_2RR after being connected to the POMs.

Following this idea, the phosphovanadomolybdate ($\{\text{PMo}_9\text{V}_7\text{O}_{44}\}$) as an oxidation motif was assembled with linear trinuclear clusters, $\{\text{M}_3\text{L}_8(\text{H}_2\text{O})_2\}$, $\text{M} = \text{Zn}, \text{Co}, \text{Ni}$, $\text{L} = 1,4\text{-di}(4\text{-}H\text{-}1,2,4\text{-triazol-4-yl})\text{benzene}$ ($p\text{-tr}_2\text{Ph}$), as the reduction motif through bridging O atoms to construct three isostructural heterocluster molecular junction photocatalysts (**RO-1**, **-2**, and **-3**, Figure 5a).³⁷ UV–vis–NIR absorption spectra showed that all three molecular junctions had a broad range of light absorption (Figure 5b). Because of the strong redox abilities and matched energy band structures, **RO-1**, **-2**, and **-3** revealed efficient CO_2RR coupling WOR in a gas–solid system (Figure 5c). The short connection distance between POMs and $\{\text{M}_3\}$ clusters with the bridging O atoms can greatly promote the charge separation and transfer. After 10-h light irradiation, **RO-1** achieved the highest CO yield ($138 \mu\text{mol g}^{-1}$ with ca. 100% selectivity). This result verifies the rationality of the design idea of HMMJ photocatalysts. Importantly, the photocatalysts still exhibit excellent photocatalytic performance in a low-concentration (30%) CO_2 atmosphere, which makes them potentially suitable for some specialized scenarios, such as the treatment of flue gas from industrial emissions. Based on this result, we changed a reduction motif $\{\text{Cu}^{\text{I}}_8(p\text{-tr}_2\text{Ph})_4\text{Cl}\}$ with stronger reducing capacity and constructed another molecular junction photocatalyst **RO-4**.³⁸ In the structure of **RO-4**, the $\{\text{Cu}^{\text{I}}_8\}$ clusters expose more active sites for CO_2RR , thus exhibiting higher photocatalytic activity as compared to **RO-1**, **-2**, and **-3**. Not only that, the multiple coordination bonds between the POMs and $\{\text{Cu}^{\text{I}}_8\}$ clusters endow **RO-4** with excellent structural stability and catalytic durability. **RO-4** can be recycled at least 15 times without significant degradation in catalytic performance.

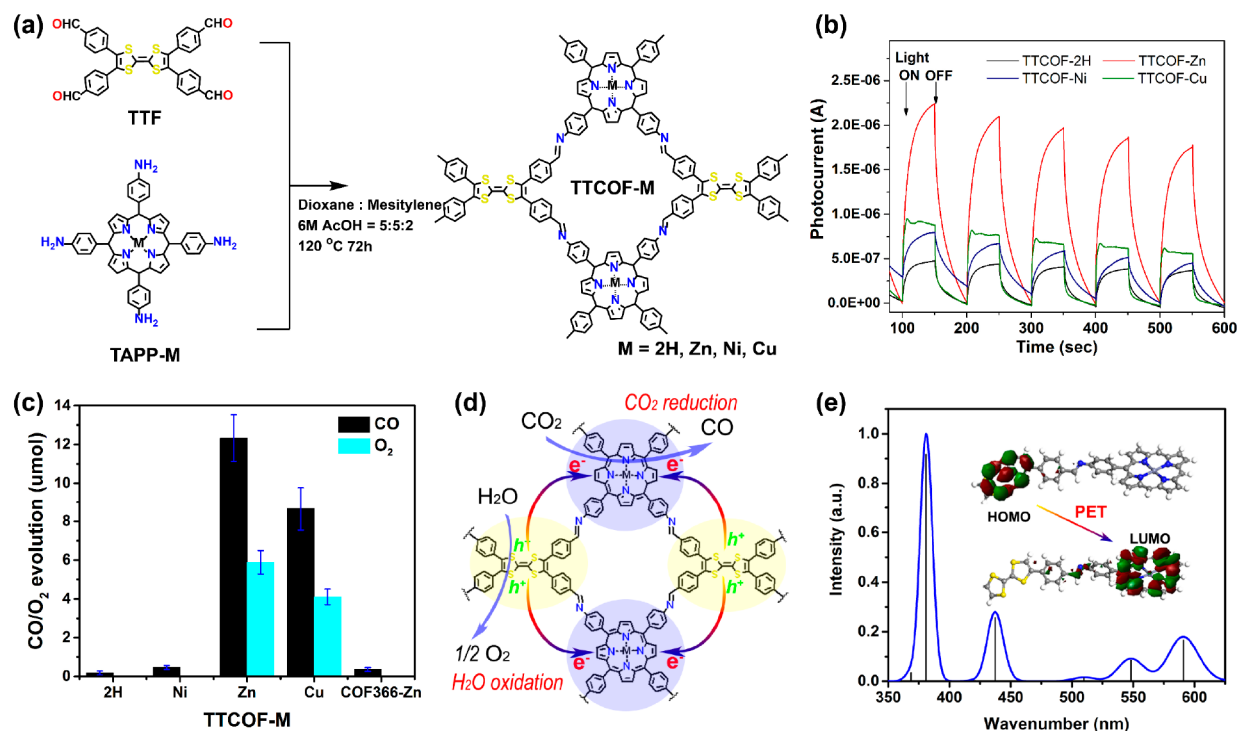


Figure 6. (a) The synthetic route and structure of TTCOFs. (b) Transient photocurrent response of TTCOFs. (c) Photocatalytic performance of TTCOFs and COF-366-Zn. (d) Mechanism of TTCOFs for artificial photosynthesis. (e) PET process between TAPP and TTF motifs from DFT simulation. Adapted with permission from ref 43. Copyright 2019 Wiley-VCH.

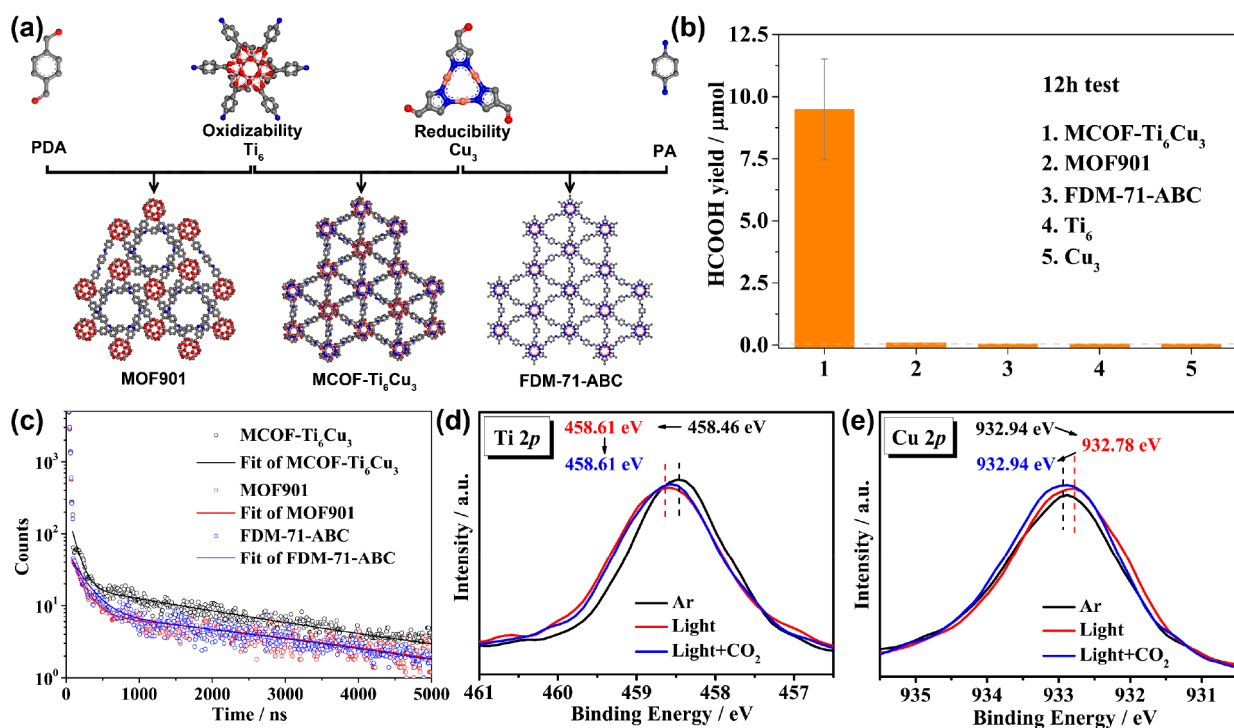


Figure 7. (a) The synthetic routes and structures of MOF-901, MCOF-Ti₆Cu₃, and FDM-71-ABC. (b) The HCOOH yields catalyzed by different samples. (c) The time-resolved fluorescence decay spectra of MOF-901, MCOF-Ti₆Cu₃, and FDM-71-ABC, respectively. High-resolution XPS spectra for (d) Ti 2p and (e) Cu 2p under different conditions. Adapted with permission from ref 2. Copyright 2022 Springer Nature.

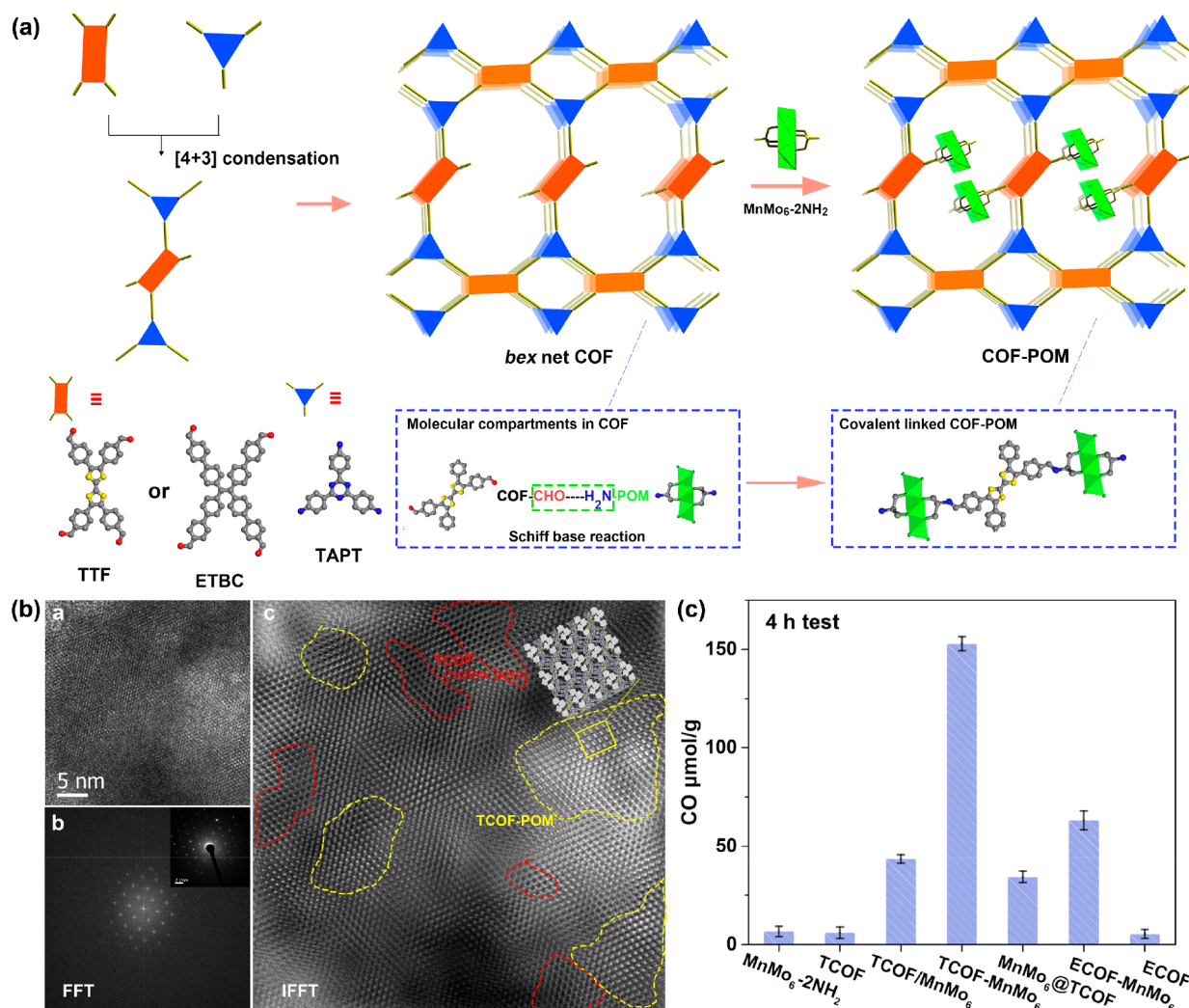


Figure 8. (a) Uniformly dispersed POM clusters in COF through covalent assembly to construct the TCOF-MnMo₆ molecular junction photocatalyst. (b) HR-TEM image of TCOF-MnMo₆. (c) The CO yields catalyzed by different photocatalysts. Adapted with permission from ref 3. Copyright 2022 American Chemical Society.

3.2. Covalent Assembly of Hetero-Motif Molecular Junction Photocatalysts

Covalent-organic frameworks (COFs) are crystalline organic porous polymers connected by molecular precursors with dynamic covalent bonds.³⁹ They have a lot of advantages such as regular structure, low density, large specific surface area, adjustable pore size, high modification, and diversified functions.^{40,41} Selecting appropriate structural motifs to construct COFs is an important means for the targeted synthesis of materials with specific properties and functions. Inspired by the molecular structure of natural chlorophyll, in recent years, COFs containing the porphyrin group as the structural motif have shown outstanding applications in the field of photocatalytic CO₂-to-CO reduction.⁴² However, it is difficult for a single porphyrin molecule to complete the WOR simultaneously. Therefore, assembling a porphyrin and another motif that can complete WOR to construct COF-based HMMJ photocatalysts is a feasible way to achieve the artificial photosynthetic overall reaction.

Hence, the metallized 5,10,15,20-tetrakis (4-aminophenyl)-porphyrato] (TAPP-M, M = 2H, Zn, Ni, Cu) and the strong

electron-donating motif 2,3,6,7-tetra (4-formylphenyl)-thiafulvalene (TTF) are connected through Schiff-base condensation to construct a series of dual-site COF molecular junction photocatalysts (TTCOF-M) containing both reducing and oxidizing capacities (Figure 6a).⁴³ Transient photocurrent tests and fluorescence spectra reveal that rapid photogenerated charge separation and migration under light irradiation occurred between TAPP-M and TTF motifs (Figure 6b). Benefiting from the well-matched energy band structures, TTCOF-Zn and TTCOF-Cu can simultaneously complete the CO₂-to-CO and H₂O-to-O₂ conversion with high selectivity and recyclability (Figure 6c). TTCOF-Zn can produce 12.33 μmol of CO with ca. 100% selectivity after a continuous 60-h illumination, which is much higher than COF-366-Zn that does not equip an oxidation motif. In addition, DFT calculation was performed to uncover the photoexcitation process. The results show that, when the TTCOFs are excited by light, the direction of photoinduced electron transfer (PET) is from TTF to TAPP-M motifs to form TTF⁺ and TAPP-M⁻, which can complete WOR and CO₂RR, respectively, due to their strong oxidizing and reducing properties (Figure 6d and e).

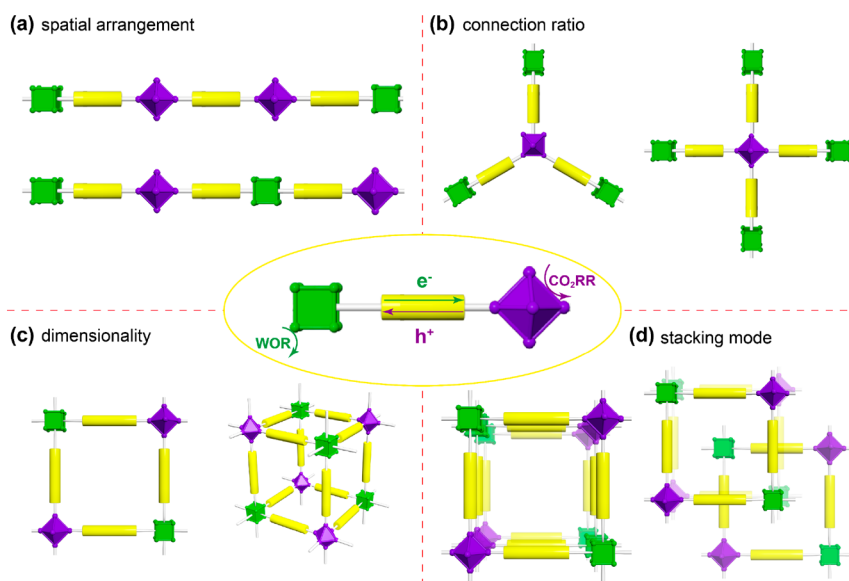


Figure 9. Several factors that can potentially influence the mode of photogenerated charge transport involved in the epitaxial growth of an isolated molecular junction to the high-dimensional structure.

In many cases, the active sites in metal-based clusters would be coordinatively saturated and inactive after the metal ions directly bond with other motifs. In this regard, two motifs can be linked by separately modifying two functional groups (such as aldehyde and amino groups) on the metal cluster that are amenable to organic coupling/condensation reactions. According to this assumption, a heterocluster molecular junction photocatalyst, labeled as **MCOF-Ti₆Cu₃**, has been intentionally assembled with an oxidative Ti-oxo cluster $\{[\text{Ti}_6\text{O}_6(\text{O}^i\text{Pr})_6(\text{AB})_6]\}$ ($\text{AB} = 4\text{-aminobenzoate}$; $\text{HO}^i\text{Pr} = \text{isopropoxide}$) and with a reductive Cu^I cluster $\{[\text{Cu}_3(\text{PyCA})_3]\}$ ($1\text{H-PyCA} = \text{pyrazolate-4-carboxaldehyde}$) through the Schiff-base condensation reaction (Figure 7a).² As a comparison, **MOF-901** and **FDM-71-ABC**, which lacked Cu₃ and Ti₆ motifs, respectively, were further synthesized. Under all-optical irradiation, **MCOF-Ti₆Cu₃** exhibited excellent activity in the conversion of CO₂ into HCOOH ($169.8 \mu\text{mol g}^{-1} \text{h}^{-1}$) with only the assistance of water (Figure 7b). **MOF-901**, **FDM-71-ABC**, and isolated Ti₆ and Cu₃ clusters were not able to accomplish the overall reaction under the same condition, which demonstrates the necessity of the existence of two motifs. The time-resolved fluorescence decay spectra indicated that the average lifetime of the photogenerated charge carriers in **MCOF-Ti₆Cu₃** is longer than those in **MOF-901** and **FDM-71-ABC** (Figure 7c). The result proved that the connection of different clusters can effectively capture and stabilize photogenerated electron–hole pairs and inhibit their recombination. Furthermore, in situ XPS spectra and DFT calculations were performed to study the migration direction of photoelectrons and the catalytic mechanism, which demonstrated that the electrons are transferred from Ti₆ to Cu₃ clusters under photoexcitation (Figure 7d and e). More importantly, the results indicated that the Cu₃ cluster occurs via the CO₂RR and the Ti₆ cluster occurs via the WOR.

3.3. Grafting Assembly of Hetero-Motif Molecular Junction Photocatalysts

Uniform dispersion of POMs in porous supports can maximize the exposure of active sites as well as inhibit their dissolution and agglomeration during catalysis.^{44,45} It can achieve more efficient

catalytic performance, which can combine the advantages of homogeneous and heterogeneous catalysis. The general methods for dispersing POMs are to integrate them in the substrates or encapsulate them in the pore/cage of porous materials. However, these methods not only make it difficult to make the clusters dispersed in space uniformly, but also face a challenge to determine the explicit structure of the clusters after interacting with the supports, limiting the building of precise structure–performance relationships. To address these problems, we demonstrated a feasible strategy for uniformly dispersing clusters in COFs.³ In constructing the COF, the reactive groups are reserved in the pores, and then the clusters are attached to the framework by grafting through covalent bonds formed by a condensation reaction. Specifically, a $[4 + 3]$ condensation reaction with TTF-4CHO and 2,4,6-tris(4-aminophenyl)-1,3,5-triazine (TAPT) was performed to obtain a COF host structure, of which two aldehyde groups in TTF-4CHO were not reacted. Subsequently, the amino-modified MnMo₆ POM ($\text{NH}_2\text{-MnMo}_6$) underwent a Schiff-base condensation reaction with the aldehyde groups, which was grafted in the pores of COF to obtain the **TCOF-MnMo₆** molecular junction photocatalyst (Figure 8a). Thanks to the reversibility of the Schiff-base reaction, the $\text{NH}_2\text{-MnMo}_6$ cluster can diffuse into the interior of the COF rather than just grafting onto the COF surface (Figure 8b). Another COF-POM molecular junction, **ECOF-MnMo₆**, was further synthesized, revealing the universality of the strategy. The photocatalytic CO₂RR was tested in a gas–solid system. After 4 h of light irradiation, **TCOF-MnMo₆** showed the highest CO₂-to-CO conversion yield of $149 \mu\text{mol g}^{-1}$, which is over 2 times higher than that of **ECOF-MnMo₆** caused by the stronger oxidizing capacity of TTF than of ETBC. In sharp contrast, the physical mixture of TCOF and MnMo₆ (**TCOF/MnMo₆**) or the POM@COF without covalent bonding showed weak activities for CO₂RR, suggesting that the direct bonding of COF and POM can promote the charge transfer and improve the properties (Figure 8c).

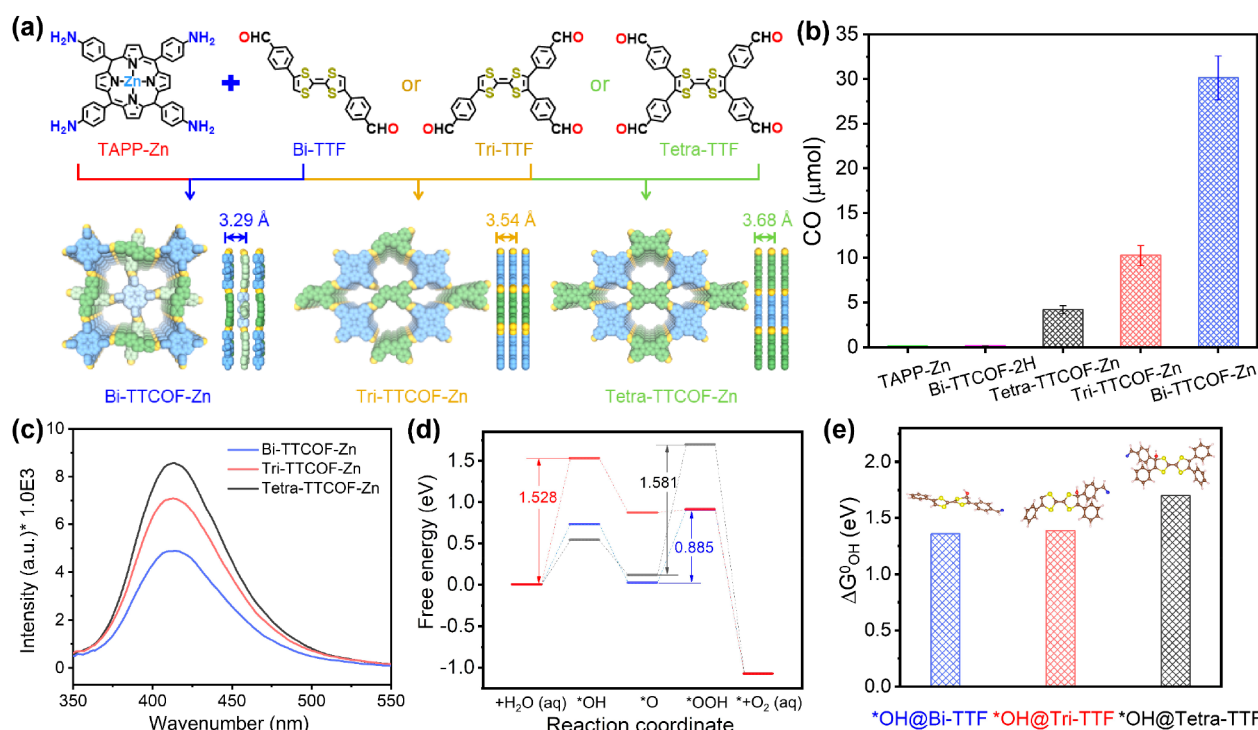


Figure 10. (a) Structures of Bi-TTCOF-Zn, Tri-TTCOF-Zn, and Tetra-TTCOF-Zn, respectively. (b) Photocatalytic CO₂-to-CO performance of TAPP-Zn, Bi-TTCOF-2H, Bi-TTCOF-Zn, Tri-TTCOF-Zn, and Tetra-TTCOF-Zn. (c) PL spectra and (d) WOR free energy diagram of Bi-TTCOF-Zn (blue), Tri-TTCOF-Zn (red), and Tetra-TTCOF-Zn (black). (e) Adsorption energy of *OH on Bi-TTCOF-Zn, Tri-TTCOF-Zn, and Tetra-TTCOF-Zn. Adapted with permission from ref 46. Copyright 2023 American Chemical Society.

3.4. Precision Regulation of Connection Patterns between Oxidation and Reduction Motifs

Photogenerated charge separation and migration are important steps in the photocatalytic process. In a single molecule of the molecular junction (containing only one oxidation and reduction motif), the photogenerated charge transfer between the hetero-motifs occurs in a manner similar to that of a semiconductor heterojunction. However, when the single molecule grows epitaxially into a high-dimensional structure, the charge transfer pathways become more complicated, which involves the interactions between more motifs. In addition, the connection patterns, such as spatial arrangement, connection ratio, and other factors, will not only directly affect the energy level structures and charge transfer efficiency of the photocatalysts, but also achieve more charge migration modes, thus affecting the photocatalytic performance (Figure 9). Due to the lack of suitable molecular models, there are only a few cases on the effect of precise regulation of connection patterns between oxidation and reduction motifs on photocatalytic efficiency.

The high designability of HMMJ photocatalysts provides an accurate visualization platform to overcome this challenge. Recently, we demonstrated the precise assembling of three heterocluster molecular junction photocatalysts using oxidative H₃PMo₁₂O₄₀ (PMo₁₂) and reductive Ni₅(bzt)₆(NO₃)₄(H₂O)₄ (Ni₅) cluster precursors in direct (*d*-OR), alternant (*a*-OR), and symmetric (*s*-OR) manners, respectively.¹ As was analyzed by energy level distributions, XPS, and in situ XPS spectroscopy, the photogenerated charge migration mode of PMo₁₂ and Ni₅ in *d*-OR is similar to that of PCI and PCII in Z-scheme heterojunctions. Further, we explored in detail the influence of the connection mode of the oxidation and reduction motifs on the charge migration and corresponding photocatalytic perform-

ance. In the solid-gas system, all three examples of photocatalysts achieved photocatalytic CO₂-to-CO reduction coupled with H₂O-to-O₂ oxidation. After a 10-h reaction, the yield of CO is *s*-OR (238.68 μmol g⁻¹) > *d*-OR (152.70 μmol g⁻¹) > *a*-OR (112.19 μmol g⁻¹), indicating that the connection modes indeed make a great influence on photocatalytic performance. In addition, all three photocatalysts have good recyclability (5 cycles) and catalytic durability (at least 200 h). Through analysis of the energy level structures and theoretical calculations, we found that the arrangement between oxidation clusters and reduction motifs can greatly affect the orbital distribution and energy level of the catalysts, and then make a giant impact on the photocatalytic reactivity. As compared to *d*-OR, the photogenerated charges of *s*-OR can transfer to a new lower vacant orbital, which is generated in the center of the R-R part to promote the photoexcited charge transfer process and inhibit the electron-hole recombination of the Ni₅ part, thereby increasing the catalytic efficiency. Nevertheless, in *a*-OR, the orbital distribution changes slightly relative to unconnected monomers Ni₅ and PMo₁₂, so as to show the weakest performance. These results are first discovered from the molecular photocatalysts and help us for the first time to propose the concept of “molecular junction photocatalysts”, which are significantly different from the reported charge transfer mode/mechanism that originated from traditional heterojunction materials.

In the previous work, benefiting from the strong electron-donating ability of TTF and the strong oxidizing property of TTF⁺, COFs containing a CO₂RR site and TTF motif achieved the effective coupling of CO₂RR and WOR. However, the overall photocatalytic efficiency is still weak. Based on these works, we hypothesized whether adjusting the interaction

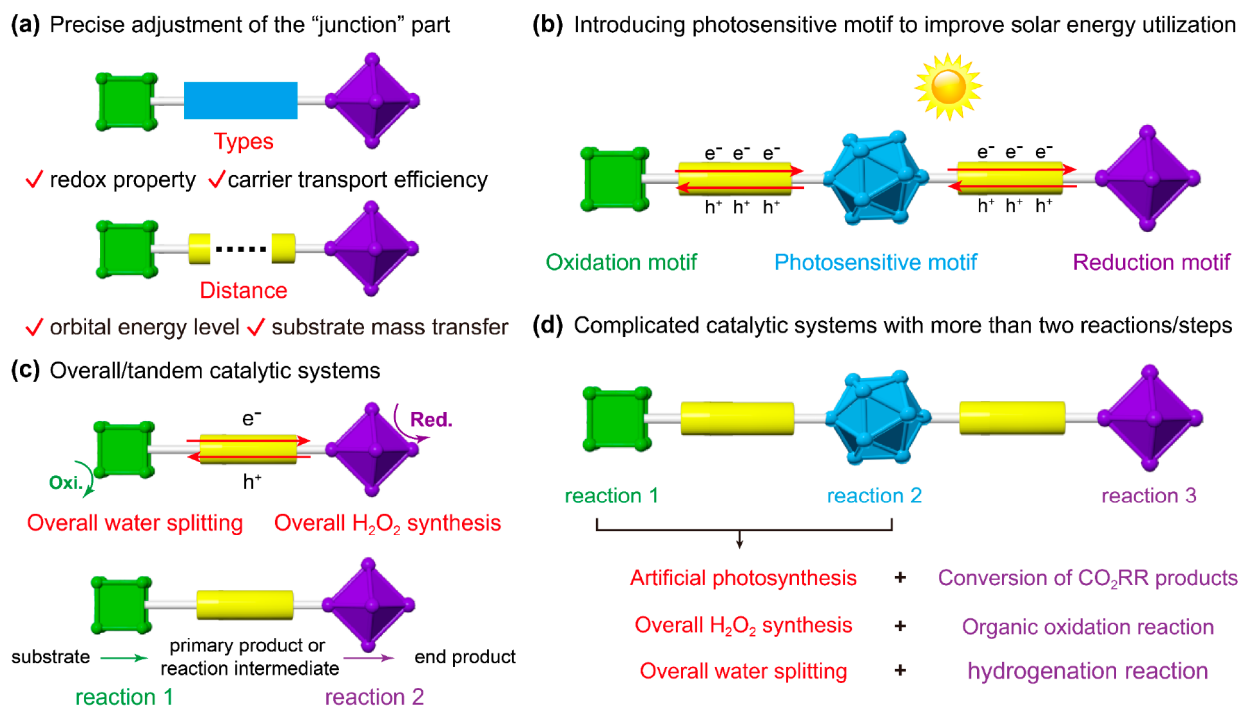


Figure 11. Strategies to improve the performance of HMMJ photocatalysts and their potential applications. (a) Future scenarios for the adjustment of the “junction” part. (b) Introducing photosensitive motifs to improve solar energy utilization. (c) More feasible overall/tandem catalytic systems that could be catalyzed by HMMJ photocatalysts. (d) Feasible cascade reactions that could be catalyzed by HMMJ photocatalysts with more motifs.

between TTF and TAPP motifs would affect the capacity of TTF to provide electrons to TAPP, thereby improving the photocatalytic performance. As a proof-of-concept, we modified the TTF basic unit to obtain ligands with different connection numbers (Bi-TTF, Tri-TTF, and Tetra-TTF) and assembled them with TAPP-Zn to obtain a series of HMMJ photocatalysts (Bi-TTCOF-Zn, Tri-TTCOF-Zn, and Tetra-TTCOF-Zn, Figure 10a).⁴⁶ This series of COFs with the same catalytic sites serve as ideal molecular models to deeply explore the impact of the connection ratio between oxidation and reduction motifs on photogenerated charge transfer and photocatalytic efficiency. Photocatalytic test results show that Bi-TTCOF-Zn exhibits the highest CO₂-to-CO conversion activity (11.56 $\mu\text{mol g}^{-1} \text{h}^{-1}$), which is beyond 2 times and 6 times higher than that of Tri-TTCOF-Zn and Tetra-TTCOF-Zn, respectively (Figure 10b). Transient photocurrent response tests and PL spectra prove that Bi-TTCOF-Zn has the highest efficiency of photogenerated charge separation and migration (Figure 10c). DFT calculation further analyzes the internal mechanism in detail. Orbital analysis shows that the HOMO and LUMO orbitals in Bi-TTCOF-Zn are more evenly distributed at TAPP-Zn and Bi-TTF as compared to those in Tri-TTCOF-Zn and Tetra-TTCOF-Zn. This allows Bi-TTCOF-Zn to exhibit stronger light absorption capabilities and increase the number of accessible sites. Subsequently, the free energy changes of the WOR process were evaluated. The results show that the different connection numbers of M-TTF greatly affect its photocatalytic activity with the ΔG_{max} for Bi-TTCOF-Zn (0.885 eV), Tri-TTCOF-Zn (1.528 eV), and Tetra-TTCOF-Zn (1.581 eV), respectively (Figure 10d). In addition, Bi-TTCOF-Zn exhibits the strongest *OH adsorption/stabilization ability. These factors combine to improve the performance of artificial photosynthesis (Figure 10e).

4. CONCLUSIONS AND PERSPECTIVES

In this Account, we have summarized the recent contributions of HMMJ photocatalysts in artificial photosynthesis. In terms of structural design, oxidative and reductive structural motifs are assembled closely and periodically, which can realize the rapid separation and migration of photogenerated electrons and holes, thereby achieving efficient coupling of CO₂RR and WOR. Based on the specific linking groups of the predetermined structural motifs, different types of HMMJ photocatalysts can be constructed through coordination and covalent assembly. Some strategies to controllably improve the reactivity of molecular junction photocatalysts, such as changing the active species, redox capacity, assembly methods, connection numbers, and other factors of the structural motifs that can achieve controllable adjustment of the light absorption, photogeneration charge separation mode, and photocatalytic activity of HMMJ photocatalysts, are summarized in detail and discussed. The clear structural information on HMMJ photocatalysts provides a visual platform for exploring the structure–performance relationships at the molecular level and provides ideas for the design and synthesis of the next generation of artificial photosynthesis catalysts. Importantly, these structure–activity relationships would be also appropriate for nanomaterial heterojunction photocatalysts, providing molecular-level insights and guidance for the design and synthesis of nano-heterojunction photocatalysts for artificial photosynthesis.

Although HMMJ photocatalysts have made initial progress in the field of artificial photosynthesis, they are still in an immature stage. Therefore, more efforts are needed for continued development, and the following key challenges must be addressed.

(1) The adjustment of linkages between oxidation and reduction motifs (i.e., the “junction” part) has been rarely studied, involving the chemical bond types, length, electron

transport ability, redox property, etc. It can make a huge impact on the carrier transport efficiency, orbital energy level of the photocatalyst, and substrate mass transfer, thereby affecting the final photocatalytic efficiency. Enhancing the redox capacity or electrical conductivity of the linkages can contribute to the efficiency of photogenerated charge separation and migration (Figure 11a).

(2) At present, the catalytic performance of many photocatalysts is limited because it is difficult to balance the redox and light absorption capacities. The structural tailorability of HMMJ photocatalysts makes it possible to coassemble photosensitive units with oxidation–reduction unit pairs. Such constructed trimotif molecular junction photocatalysts can realize the enhancement of solar energy utilization (Figure 11b).

(3) In addition to artificial photosynthesis, these novel bifunctional photocatalysts that combine both oxidation and reduction motifs also have greater potential to be applied to more photocatalytic overall reaction systems (such as overall water splitting or H_2O_2 photosynthesis reactions and so on). It requires the design of more structural motifs and the development of more advanced strategies (for example, cocrystallization of the two motifs with a short distance and strong interactions that allow rapid charge transfer) to assemble them into a HMMJ photocatalyst. In addition, the catalysts constructed by rationally assembling multistructural motifs are also suitable for tandem catalysis, which can further reduce the generated 2e^- products or convert them into organics when constructing HMMJ photocatalysts with a CO_2RR motif and another catalytic motif (Figure 11c).

(4) In the photocatalytic overall reaction systems, it is a great challenge to directly utilize the generated low-value products to prepare high-value chemicals. It requires the catalysts to not only complete the coupling of the oxidation and the reduction reactions, but also cascade the next catalytic reaction. The assembly of three (or more) structural motifs to construct HMMJ photocatalysts is expected to overcome this challenge and directly utilize the generated CO , HCOOH , H_2 , or H_2O_2 for the preparation of fine chemicals. Notably, this is a green pathway to prepare chemicals using water as a clean H and O source, which is of great scientific significance (Figure 11d).

In view of the high degree of designability and tunability of HMMJ photocatalysts, we firmly believe that this new type of multifunctional catalyst can have bright prospects in various fields of complex, multistep photocatalysis, electrocatalysis, thermal catalysis, and other catalytic systems.

AUTHOR INFORMATION

Corresponding Author

Ya-Qian Lan – School of Chemistry, South China Normal University, Guangzhou 510006, People's Republic of China; orcid.org/0000-0002-2140-7980; Email: yqlan@m.scnu.edu.cn

Authors

Lei Zhang – School of Chemistry, South China Normal University, Guangzhou 510006, People's Republic of China; orcid.org/0000-0001-5447-1631

Jiang Liu – School of Chemistry, South China Normal University, Guangzhou 510006, People's Republic of China; orcid.org/0000-0002-2596-4928

Complete contact information is available at:

<https://pubs.acs.org/10.1021/acs.accounts.3c00751>

Author Contributions

L.Z. contributed to the conceptualization, funding acquisition, investigation, software, writing-original draft, writing-review, and editing. J.L. contributed to the conceptualization, supervision, writing-review, and editing. Y.-Q.L. contributed to the conceptualization, funding acquisition, supervision, writing-original draft, writing-review, and editing.

Notes

The authors declare no competing financial interest.

Biographies

Lei Zhang received his Ph.D. degree in Inorganic Chemistry from Nanjing Normal University in 2021. In 2021, he joined South China Normal University as a research assistant professor. His research focuses on the design and construction of metal cluster-based coordination polymers for photocatalysis and electrocatalysis.

Jiang Liu obtained his Ph.D. degree from the School of Chemistry and Chemical Engineering, Sun Yat-Sen University, in 2016. Since 2022, he has been a professor at South China Normal University. His research interest focuses on the development of molecular-based metal cluster and metal–organic crystalline materials applied in energy storage and conversion, proton conductivity, and photo/electric heterogeneous catalysis.

Ya-Qian Lan received his Ph.D. degree (2009) from the Faculty of Chemistry, Northeast Normal University. In 2010, he joined the National Institute of Advanced Industrial Science and Technology (AIST, Japan) as a JSPS postdoctoral fellow. Now, he is a professor at South China Normal University. His research interests focus on the application of polyoxometalate-based composite materials in energy storage and conversion and porous metal–organic frameworks for applications in catalysis and proton conduction.

ACKNOWLEDGMENTS

We acknowledge support from the National Natural Science Foundation of China (nos. 22201082, 22225109, and 92061101), the Guangdong Basic and Applied Basic Research Foundation (no. 2021A1515110429), and the project funded by the China Postdoctoral Science Foundation (nos. 2022M721216 and 2023T160235).

REFERENCES

- (1) Zhang, L.; Li, R.-H.; Li, X.-X.; Liu, J.; Guan, W.; Dong, L.-Z.; Li, S.-L.; Lan, Y.-Q. Molecular oxidation–reduction junctions for artificial photosynthetic overall reaction. *Proc. Natl. Acad. Sci. U. S. A.* **2022**, *119*, No. e2210550119.
- (2) Zhou, J.; Li, J.; Kan, L.; Zhang, L.; Huang, Q.; Yan, Y.; Chen, Y.; Liu, J.; Li, S.-L.; Lan, Y.-Q. Linking oxidative and reductive clusters to prepare crystalline porous catalysts for photocatalytic CO_2 reduction with H_2O . *Nat. Commun.* **2022**, *13*, 4681.
- (3) Lu, M.; Zhang, M.; Liu, J.; Yu, T.-Y.; Chang, J.-N.; Shang, L.-J.; Li, S.-L.; Lan, Y.-Q. Confining and Highly Dispersing Single Polyoxometalate Clusters in Covalent Organic Frameworks by Covalent Linkages for CO_2 Photoreduction. *J. Am. Chem. Soc.* **2022**, *144*, 1861–1871.
- (4) Dong, L.-Z.; Zhang, L.; Liu, J.; Huang, Q.; Lu, M.; Ji, W.-X.; Lan, Y.-Q. Stable Heterometallic Cluster-Based Organic Framework Catalysts for Artificial Photosynthesis. *Angew. Chem., Int. Ed.* **2020**, *59*, 2659–2663.
- (5) Ding, M.; Flaig, R. W.; Jiang, H.-L.; Yaghi, O. M. Carbon capture and conversion using metal–organic frameworks and MOF-based materials. *Chem. Soc. Rev.* **2019**, *48*, 2783–2828.
- (6) Li, J.; Huang, H.; Xue, W.; Sun, K.; Song, X.; Wu, C.; Nie, L.; Li, Y.; Liu, C.; Pan, Y.; Jiang, H.-L.; Mei, D.; Zhong, C. Self-adaptive dual-

metal-site pairs in metal-organic frameworks for selective CO₂ photoreduction to CH₄. *Nat. Catal.* **2021**, *4*, 719–729.

(7) Yin, H.-Q.; Zhang, Z.-M.; Lu, T.-B. Ordered Integration and Heterogenization of Catalysts and Photosensitizers in Metal-/Covalent-Organic Frameworks for Boosting CO₂ Photoreduction. *Acc. Chem. Res.* **2023**, *56*, 2676–2687.

(8) Sakimoto, K. K.; Wong, A. B.; Yang, P. Self-photosensitization of nonphotosynthetic bacteria for solar-to-chemical production. *Science* **2016**, *351*, 74–77.

(9) Yuan, L.; Qi, M.-Y.; Tang, Z.-R.; Xu, Y.-J. Coupling Strategy for CO₂ Valorization Integrated with Organic Synthesis by Heterogeneous Photocatalysis. *Angew. Chem., Int. Ed.* **2021**, *60*, 21150–21172.

(10) Liu, H.; Chen, Y.; Li, H.; Wan, G.; Feng, Y.; Wang, W.; Xiao, C.; Zhang, G.; Xie, Y. Construction of Asymmetrical Dual Jahn-Teller Sites for Photocatalytic CO₂ Reduction. *Angew. Chem., Int. Ed.* **2023**, *62*, No. e202304562.

(11) Guo, Q.; Liang, F.; Li, X.-B.; Gao, Y.-J.; Huang, M.-Y.; Wang, Y.; Xia, S.-G.; Gao, X.-Y.; Gan, Q.-C.; Lin, Z.-S.; Tung, C.-H.; Wu, L.-Z. Efficient and Selective CO₂ Reduction Integrated with Organic Synthesis by Solar Energy. *Chem.* **2019**, *5*, 2605–2616.

(12) Listorti, A.; Durrant, J.; Barber, J. Solar to fuel. *Nat. Mater.* **2009**, *8*, 929–930.

(13) Wang, Q.; Warnan, J.; Rodríguez-Jiménez, S.; Leung, J. J.; Kalathil, S.; Andrei, V.; Domen, K.; Reisner, E. Molecularly engineered photocatalyst sheet for scalable solar formate production from carbon dioxide and water. *Nat. Energy* **2020**, *5*, 703–710.

(14) Shi, Y.; Li, J.; Mao, C.; Liu, S.; Wang, X.; Liu, X.; Zhao, S.; Liu, X.; Huang, Y.; Zhang, L. Van Der Waals gap-rich BiOCl atomic layers realizing efficient, pure-water CO₂-to-CO photocatalysis. *Nat. Commun.* **2021**, *12*, 5923.

(15) Yin, S.; Zhao, X.; Jiang, E.; Yan, Y.; Zhou, P.; Huo, P. Boosting water decomposition by sulfur vacancies for efficient CO₂ photoreduction. *Energy Environ. Sci.* **2022**, *15*, 1556–1562.

(16) Wang, W.-N.; An, W.-J.; Ramalingam, B.; Mukherjee, S.; Niedzwiedzki, D. M.; Gangopadhyay, S.; Biswas, P. Size and Structure Matter: Enhanced CO₂ Photoreduction Efficiency by Size-Resolved Ultrafine Pt Nanoparticles on TiO₂ Single Crystals. *J. Am. Chem. Soc.* **2012**, *134*, 11276–11281.

(17) Zhang, L.; Li, R.-H.; Li, X.-X.; Wang, S.; Liu, J.; Hong, X.-X.; Dong, L.-Z.; Li, S.-L.; Lan, Y.-Q. Photocatalytic aerobic oxidation of C(sp³)-H bonds. *Nat. Commun.* **2024**, *15*, 537.

(18) Luo, Z.; Ye, X.; Zhang, S.; Xue, S.; Yang, C.; Hou, Y.; Xing, W.; Yu, R.; Sun, J.; Yu, Z.; Wang, X. Unveiling the charge transfer dynamics steered by built-in electric fields in BiOBr photocatalysts. *Nat. Commun.* **2022**, *13*, 2230.

(19) Low, J.; Yu, J.; Jaroniec, M.; Wageh, S.; Al-Ghamdi, A. A. Heterojunction Photocatalysts. *Adv. Mater.* **2017**, *29*, 1601694.

(20) Wang, H.; Zhang, L.; Chen, Z.; Hu, J.; Li, S.; Wang, Z.; Liu, J.; Wang, X. Semiconductor heterojunction photocatalysts: design, construction, and photocatalytic performances. *Chem. Soc. Rev.* **2014**, *43*, 5234–5244.

(21) Wang, Y.; Zhang, Z.; Zhang, L.; Luo, Z.; Shen, J.; Lin, H.; Long, J.; Wu, J. C. S.; Fu, X.; Wang, X.; Li, C. Visible-Light Driven Overall Conversion of CO₂ and H₂O to CH₄ and O₂ on 3D-SiC@2D-MoS₂ Heterostructure. *J. Am. Chem. Soc.* **2018**, *140*, 14595–14598.

(22) Yoshino, S.; Iwase, A.; Yamaguchi, Y.; Suzuki, T. M.; Morikawa, T.; Kudo, A. Photocatalytic CO₂ Reduction Using Water as an Electron Donor under Visible Light Irradiation by Z-Scheme and Photoelectrochemical Systems over (CuGa)_{0.5}ZnS₂ in the Presence of Basic Additives. *J. Am. Chem. Soc.* **2022**, *144*, 2323–2332.

(23) Wang, Y.; Shang, X.; Shen, J.; Zhang, Z.; Wang, D.; Lin, J.; Wu, J. C. S.; Fu, X.; Wang, X.; Li, C. Direct and indirect Z-scheme heterostructure-coupled photosystem enabling cooperation of CO₂ reduction and H₂O oxidation. *Nat. Commun.* **2020**, *11*, 3043.

(24) Yu, S.; Kim, Y. H.; Lee, S. Y.; Song, H. D.; Yi, J. Hot-Electron-Transfer Enhancement for the Efficient Energy Conversion of Visible Light. *Angew. Chem., Int. Ed.* **2014**, *53*, 11203–11207.

(25) Li, N.; Chen, X.; Wang, J.; Liang, X.; Ma, L.; Jing, X.; Chen, D.-L.; Li, Z. ZnSe Nanorods-CsSnCl₃ Perovskite Heterojunction Composite for Photocatalytic CO₂ Reduction. *ACS Nano* **2022**, *16*, 3332–3340.

(26) Lin, H.; Liu, Y.; Wang, Z.; Ling, L.; Huang, H.; Li, Q.; Cheng, L.; Li, Y.; Zhou, J.; Wu, K.; Zhang, J.; Zhou, T. Enhanced CO₂ Photoreduction through Spontaneous Charge Separation in End-Capping Assembly of Heterostructured Covalent-Organic Frameworks. *Angew. Chem., Int. Ed.* **2022**, *61*, No. e202214142.

(27) Bian, J.; Zhang, Z.; Feng, J.; Thangamuthu, M.; Yang, F.; Sun, L.; Li, Z.; Qu, Y.; Tang, D.; Lin, Z.; Bai, F.; Tang, J.; Jing, L. Energy Platform for Directed Charge Transfer in the Cascade Z-Scheme Heterojunction: CO₂ Photoreduction without a Cocatalyst. *Angew. Chem., Int. Ed.* **2021**, *60*, 20906–20914.

(28) Jiang, Y.; Liao, J.-F.; Chen, H.-Y.; Zhang, H.-H.; Li, J.-Y.; Wang, X.-D.; Kuang, D.-B. All-Solid-State Z-Scheme α -Fe₂O₃/Amine-RGO/CsPbBr₃ Hybrids for Visible-Light-Driven Photocatalytic CO₂ Reduction. *Chem.* **2020**, *6*, 766–780.

(29) Xu, Q.; Zhang, L.; Cheng, B.; Fan, J.; Yu, J. S-Scheme Heterojunction Photocatalyst. *Chem.* **2020**, *6*, 1543–1559.

(30) Miao, Z.; Wang, Q.; Zhang, Y.; Meng, L.; Wang, X. In situ construction of S-scheme AgBr/BiOBr heterojunction with surface oxygen vacancy for boosting photocatalytic CO₂ reduction with H₂O. *Appl. Catal., B* **2022**, *301*, 120802.

(31) Liu, J.; Liu, Y.; Liu, N.; Han, Y.; Zhang, X.; Huang, H.; Lifshitz, Y.; Lee, S.-T.; Zhong, J.; Kang, Z. Metal-free efficient photocatalyst for stable visible water splitting via a two-electron pathway. *Science* **2015**, *347*, 970–974.

(32) Dong, P.; Xu, X.; Luo, R.; Yuan, S.; Zhou, J.; Lei, J. Postsynthetic Annulation of Three-Dimensional Covalent Organic Frameworks for Boosting CO₂ Photoreduction. *J. Am. Chem. Soc.* **2023**, *145*, 15473–15481.

(33) Li, N.; Liu, J.; Liu, J.-J.; Dong, L.-Z.; Li, S.-L.; Dong, B.-X.; Kan, Y.-H.; Lan, Y.-Q. Self-Assembly of a Phosphate-Centered Polyoxo-Titanium Cluster: Discovery of the Heteroatom Keggin Family. *Angew. Chem., Int. Ed.* **2019**, *58*, 17260–17264.

(34) Huang, Q.; Liu, J.; Feng, L.; Wang, Q.; Guan, W.; Dong, L.-Z.; Zhang, L.; Yan, L.-K.; Lan, Y.-Q.; Zhou, H.-C. Multielectron transportation of polyoxometalate-grafted metalloporphyrin coordination frameworks for selective CO₂-to-CH₄ photoconversion. *Natl. Sci. Rev.* **2020**, *7*, 53–63.

(35) Du, J.; Ma, Y.-Y.; Cui, W.-J.; Zhang, S.-M.; Han, Z.-G.; Li, R.-H.; Han, X.-Q.; Guan, W.; Wang, Y.-H.; Li, Y.-Q.; Liu, Y.; Yu, F.-Y.; Wei, K.-Q.; Tan, H.-Q.; Kang, Z.-H.; Li, Y.-G. Unraveling photocatalytic electron transfer mechanism in polyoxometalate-encapsulated metal-organic frameworks for high-efficient CO₂ reduction reaction. *Appl. Catal., B* **2022**, *318*, 121812.

(36) Yin, Q.; Tan, J. M.; Besson, C.; Geletii, Y. V.; Musaev, D. G.; Kuznetsov, A. E.; Luo, Z.; Hardcastle, K. I.; Hill, C. L. A Fast Soluble Carbon-Free Molecular Water Oxidation Catalyst Based on Abundant Metals. *Science* **2010**, *328*, 342–345.

(37) Li, X.-X.; Zhang, L.; Liu, J.; Yuan, L.; Wang, T.; Wang, J.-Y.; Dong, L.-Z.; Huang, K.; Lan, Y.-Q. Design of Crystalline Reduction-Oxidation Cluster-Based Catalysts for Artificial Photosynthesis. *JACS Au* **2021**, *1*, 1288–1295.

(38) Li, X.-X.; Zhang, L.; Yuan, L.; Wang, T.; Dong, L.-Z.; Huang, K.; Liu, J.; Lan, Y.-Q. Constructing crystalline redox catalyst to achieve efficient CO₂ photoreduction reaction in water vapor. *Chem. Eng. J.* **2022**, *442*, 136157.

(39) Diercks, C. S.; Yaghi, O. M. The atom, the molecule, and the covalent organic framework. *Science* **2017**, *355*, No. eaal1585.

(40) Lu, M.; Zhang, M.; Liu, J.; Chen, Y.; Liao, J.-P.; Yang, M.-Y.; Cai, Y.-P.; Li, S.-L.; Lan, Y.-Q. Covalent Organic Framework Based Functional Materials: Important Catalysts for Efficient CO₂ Utilization. *Angew. Chem., Int. Ed.* **2022**, *61*, No. e202200003.

(41) Geng, K.; He, T.; Liu, R.; Dalapati, S.; Tan, K. T.; Li, Z.; Tao, S.; Gong, Y.; Jiang, Q.; Jiang, D. Covalent Organic Frameworks: Design, Synthesis, and Functions. *Chem. Rev.* **2020**, *120*, 8814–8933.

(42) Ding, J.; Guan, X.; Lv, J.; Chen, X.; Zhang, Y.; Li, H.; Zhang, D.; Qiu, S.; Jiang, H.-L.; Fang, Q. Three-Dimensional Covalent Organic

Frameworks with Ultra-Large Pores for Highly Efficient Photocatalysis. *J. Am. Chem. Soc.* **2023**, *145*, 3248–3254.

(43) Lu, M.; Liu, J.; Li, Q.; Zhang, M.; Liu, M.; Wang, J.-L.; Yuan, D.-Q.; Lan, Y.-Q. Rational Design of Crystalline Covalent Organic Frameworks for Efficient CO₂ Photoreduction with H₂O. *Angew. Chem., Int. Ed.* **2019**, *58*, 12392–12397.

(44) Liu, L.; Corma, A. Confining isolated atoms and clusters in crystalline porous materials for catalysis. *Nat. Rev. Mater.* **2021**, *6*, 244–263.

(45) Dong, C.; Li, Y.; Cheng, D.; Zhang, M.; Liu, J.; Wang, Y.-G.; Xiao, D.; Ma, D. Supported Metal Clusters: Fabrication and Application in Heterogeneous Catalysis. *ACS Catal.* **2020**, *10*, 11011–11045.

(46) Li, Q.; Chang, J.-N.; Wang, Z.; Lu, M.; Guo, C.; Zhang, M.; Yu, T.-Y.; Chen, Y.; Li, S.-L.; Lan, Y.-Q. Modulated Connection Modes of Redox Units in Molecular Junction Covalent Organic Frameworks for Artificial Photosynthetic Overall Reaction. *J. Am. Chem. Soc.* **2023**, *145*, 23167–23175.